Polaron dynamics in two types of long oligothiophenes revealed by *Q*- and *X*-band ESR measurements

Katsuichi Kanemoto,[1,*] Ko Furukawa,[2] Nobukazu Negishi,[3] Yoshio Aso,[3] and Tetsuo Otsubo[4]
[1]*Department of Physics, Graduate School of Science, Osaka City University, 3-3-138 Sugimoto, Sumiyoshi-ku, Osaka 558-8585, Japan*
[2]*Institute for Molecular Science, Nishigonaka 38, Myodaiji, Okazaki, 444-8585 Aichi, Japan*
[3]*The Institute of Scientific and Industrial Research, Osaka University, Ibaraki, Osaka 567-0047, Japan*
[4]*Department of Applied Chemistry, Graduate School of Engineering, Hiroshima University, Higashi-hiroshima 739-8527, Japan*
(Received 19 January 2007; revised manuscript received 11 May 2007; published 5 October 2007)

The polaron dynamics has been investigated through the *X*- and *Q*-band ESR measurements for two types of iodine-doped long oligothiophenes, the 20-mer with octyl substituents (*o*-20T) and the 16-mer with hexyl substituents (*h*-16T). *o*-20T, used as a model compound of conjugated polymers with crystalline grains, gives anisotropic ESR spectra attributed to *g* anisotropy at low temperatures. The anisotropic spectra are found to be brought by polarons moving within the crystalline grains consisting of parallel chains. The anisotropy is shown to decrease with increasing temperature. This provides definite evidence that the polarons transfer among some grains by the assist of temperature. In contrast, *h*-16T, used as a model of the polymers with amorphous morphology, gives almost isotropic ESR spectra even in the *Q*-band measurement. This feature of *h*-16T is explained to be caused by a rapid interchain transfer of polarons. Spectral simulations performed for obtained spectra reveal that the ESR linewidth in the *Q*-band measurement is larger than that in the *X* band for both oligothiophenes. The difference of the linewidth is analyzed by a simplified motional narrowing model in order to draw the information of polaron dynamics. Analyses for *o*-20T show that the intergrain motion almost follows the variable range hopping model. The interchain motion in *h*-16T is found to have a much weaker temperature dependence than the intergrain motion in *o*-20T. This result suggests that the interchain dynamics of *h*-16T revealed by the ESR technique includes a variety of processes of motion.

DOI: 10.1103/PhysRevB.76.155205 PACS number(s): 73.61.Ph, 76.30.−v

I. INTRODUCTION

High conductivity achieved in heavily doped conjugated polymers has attracted much attention due to their potential application to semiconductor devices. Indeed, a field effect transistor using conjugated polymers has been realized with the use of the conductive carriers that have similar electronic structures with the doped sates.[1] In the conducting event, polaron species with a 1/2 electron spin have been considered to be one of possible carriers.[2] The dynamics of the polaron has thus been studied on the basis of ESR techniques.[3,4] Particularly, the ESR spectroscopy has also been applied to investigating polarons generated at photoexcitations[5] and in device performances.[6,7] It is, however, difficult to derive decisive information concerning the polaron dynamics from spectra measured with only a conventional ESR technique. One of the reasons is that the spectrum of the doped conjugated polymer is usually averaged due to a rapid polaron motion and gives no appreciable spectral structures containing static information such as a hyperfine coupling constant and spectral anisotropic parameters. In addition, there are some paramagnetic components such as defects or trapped species that can coexist with polarons[8] and it makes spectral information more ambiguous. To deal with these problems, advanced ESR techniques have been adopted. Above all, treatments on the basis of the frequency dependences of ESR linewidth[3,4] and the electron spin relaxation times measured by a pulsed ESR technique[9,10] have been proved to be effective to investigate the polaron dynamics in conjugated polymers.

In contrast, the use of advanced ESR techniques is not sufficient to account for the polaron dynamics of polymer samples, because such samples usually have some uncertain structural elements. Particularly, with respect to a chain length, when there is a degree of distribution in the chain length, obtained spectra can be made inhomogeneously broadened. From this point, the use of materials with a well-defined chain length, oligomers, is one of the effective ways for explicitly exploring the spin dynamics. Conjugated oligomers have been used as a model compound of conjugated polymers, particularly on the basis of oligothiophenes.[11,12] Then, a short length of oligomers, mainly up to the 6-mer, were mostly adopted. Recently, however, long sizes of alkyl-substituted oligothiophenes over the 10-mer (the 48-mer at the longest[13]) have been developed[13–15] and shown to be more desirable models of polythiophene (PT).[13–17]

Previously, we reported briefly the ESR results of doped 13- and 20-mer oligothiophenes with octyl substituents.[18] Their polarons generated by iodine doping were then concluded to move within aggregates consisted of parallel chains. Related to this, the octyl-substituted oligomers have recently been ascertained to generate stacked lamella structures in a self-assembling way in the nondoped state.[19] This is consistent with the previous ESR results that suggested the presence of crystalline grains,[18] although its structure could vary by doping as reported previously.[20] In this paper, the polaron dynamics is investigated in detail not only for the 20-mer oligomer with octyl substituents but also for the 16-mer oligothiophene with hexyl substituents. In a usual polymer solid film, two types of morphologies exist. The first one is a crystalline that consists of oriented chain molecules with strong interchain couplings. A prototype of having such a morphology is regioregular poly(alkylthiophenes) (PATs)

with head-to-tail coupled substituents.[21] The other type is an amorphous morphology consisting primarily of chains with weak interchain couplings. Most of polymer films are sorted into this type. The 16-mer oligomer used in this study has a morphology of amorphous type in the solid film. We therefore treat these two types of long oligothiophenes as prototypes of polymers with each morphology in the solid film and investigate their polaron dynamics. In the previous paper, the presence of *g* anisotropy was identified for the ESR spectra of the 20-mer oligomer.[18] We here focus on features in *g* anisotropy for investigating the polaron dynamics. In order to make the information on spectral *g* anisotropy clearer, we adopted a *Q*-band ESR technique with higher frequency (~36 GHz) than a conventional *X*-band ESR (~9 GHz). We show that analyses through the comparison of ESR spectra between *X*- and *Q*-band measurements enable us to extract the information on interchain or intergrain hopping processes that are directly associated with temperature dependences of conductivity. Our consequences would be meaningful for the application of ESR techniques to evaluating photophysical and device properties as well.

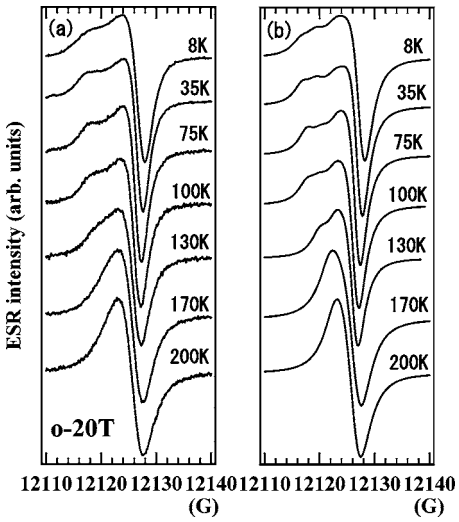

FIG. 1. (a) ESR spectra in the *Q*-band measurements of the 20-mer oligothiophene with octyl substituents (*o*-20T) measured at various temperatures. (b) Simulated spectra for the spectra in (a).

II. EXPERIMENT

Oligomer samples used in this study are the hexyl-substituted 16-mer and the octyl-substituted 20-mer α-linked oligothiophenes (hereafter, *h*-16T and *o*-20T, respectively). The syntheses of these oligomers as well as their fundamental properties were reported previously.[13–15] We prepared ESR samples by exposing the neutral films cast from their chloroform solutions to excess iodine vapor in half an hour. About 20% of thiophene rings were estimated to be doped by I_3^- ions through elemental analyses.[15] The casting films were prepared at the inside bottom of an ESR tube (2 or 3 mm diameter) for good heat contact with cooling He gas flowing outside the tube in the low temperature measurements. The tubes were evacuated ($<10^{-2}$ Torr) in order to prevent the effect of linewidth broadening due to residual molecular oxygen.[22,23] ESR measurements were carried out with the Bruker E680 for *X* band (9.6 GHz) and the E500 spectrometers for *Q* band (34 GHz). ESR spectra in *X*- and *Q*-band measurements were recorded in the same day (within 24 h) using the identical batch sample for each oligomer, in order to precisely compare the spectra. It was previously reported that *g* factors in the flat film of doped PATs vary depending on the geometry of the film plane to the static magnetic field.[24] In our case, the films were grown semispherically in the ESR tube with a thickness of some micrometers and did not give appreciable *g* shifts nor line shape variations when the tube was rotated. This suggests that spectra were obtained from a randomly oriented system. ESR signals were stable over several months after sealed in the evacuated tube. ESR signals of the oligomer samples before doping were unobservable or negligible compared to those after doping. This indicates that observed ESR signals after doping originate from the polaron species that were generated from the iodine doping. The ESR linewidth after doping in a different batch of samples was somewhat different at higher temperatures around room temperature in both oligomers. It would be due to some morphology differences among different batches of samples. However, the difference in the linewidth was appreciably reduced with decreasing temperature and trends in the temperature dependences of linewidth were similar among different batches of samples. The conductivity of *h*-16T after iodine doping measured by a four-probe method was in the order of 10^0 at room temperature, which is the same order of magnitude as that of *o*-20T reported previously.[15]

III. RESULTS

It was recently proved by an x-ray diffraction (XRD) measurement that *o*-20T generates crystalline grains with spacing of 15.5 Å in the solid film.[19] In contrast, we did not observe appreciable diffraction peaks demonstrating the presence of crystalline grains in the XRD measurement for the solid film of *h*-16T. These findings confirm that *o*-20T and *h*-16T oligomers are good prototypes of conjugated polymers with crystalline grains and with an amorphous phase, respectively. Both *o*-20T and *h*-16T gave strong ESR signals after iodine doping. The ESR spectra of *o*-20T exhibited anisotropic line shape in *Q*-band measurements as well as in *X*-band one as has been reported previously.[18] The anisotropy was highly enhanced in *Q* band. Some examples of the *Q*-band spectra are shown in Fig. 1. The result that the spectral anisotropy is enhanced in a higher frequency ESR demonstrates that the anisotropy is brought by *g* factor. The spectra in Fig. 1 further indicate that the *g* anisotropy is reduced with increasing temperature. This trend was previously reported for the *X*-band spectra of the *o*-20T sample,[18] but it is more clearly displayed by adopting the *Q*-band ESR. Figure 2 shows the ESR spectra of *h*-16T in *Q* band measured at 35, 100, and 200 K. Unlike the case of *o*-20T, the spectra of *h*-16T do not exhibit explicit anisotropy, exclusive of the spectrum at 35 K with small anisotropy. The difference in the degree of spectral anisotropy between *h*-16T and

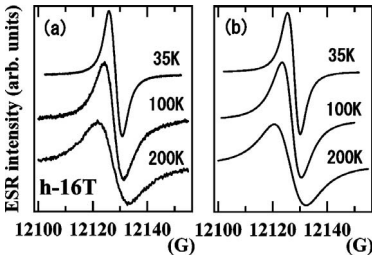

FIG. 2. (a) ESR spectra in the Q-band measurements of the 16-mer oligothiophene with hexyl substituents (h-16T) measured at 35, 100, and 200 K. (b) Simulated spectra for the spectra in (a).

o-20T suggests that the observed anisotropy in o-20T is due to its crystalline morphology in the film.

The crystalline regions in o-20T are expected to be randomly oriented within the film. Therefore the spectra in o-20T, as well as in h-16T with an amorphous morphology, can be simulated with a powder pattern. Spectral simulations for the observed ESR spectra were thus performed by assuming a powder pattern. Examples of simulated spectra are shown in Figs. 1 and 2 for o-20T and h-16T, respectively. A Lorentzian curve gave the best fits and was used as constituent packets of a powder pattern spectrum in the simulation. Simulation parameters are then axially symmetric g factors, $g_{\|}$ and $g_{\perp}$, and a Lorentzian linewidth. In the case of o-20T, two components differing only in $g_{\|}$ were used to fit observed spectra. This suggests that there would be two or more paramagnetic species with different magnetic environments in the solid film. The $g_{\|}$ of o-20T was thus represented by weighted average.

The values of $g_{\|}$ and $g_{\perp}$ obtained from the spectral simulations are plotted in Figs. 3 and 4 for o-20T and h-16T, respectively. The result in Fig. 3 indicates that the g anisotropy, defined by $g_{\|}-g_{\perp}$, of o-20T gradually decreases with increasing temperature, while the mean g value $g_{\mathrm{av}}[=1/3(g_{\|}+2\times g_{\perp})]$ is almost independent of temperature. As mentioned above, the observed g anisotropy in o-20T is associated with its crystalline morphology in the film. This means that the electron spins present in crystalline regions give rise to anisotropic ESR spectra with a powder pattern. Therefore the decrease in the g anisotropy identified at

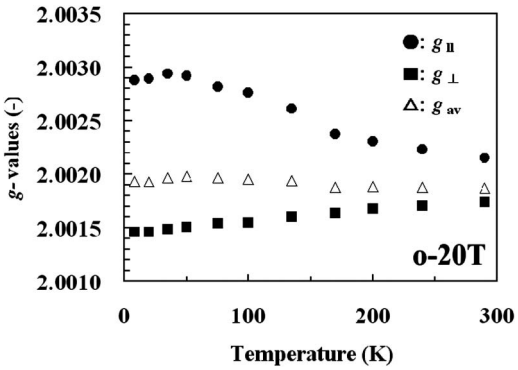

FIG. 3. Temperature dependences of $g_{\|}$, $g_{\perp}$, and g_{av} $[=1/3(g_{\|}+2\times g_{\perp})]$ for o-20T determined from spectral fits assuming an axially symmetric powder pattern.

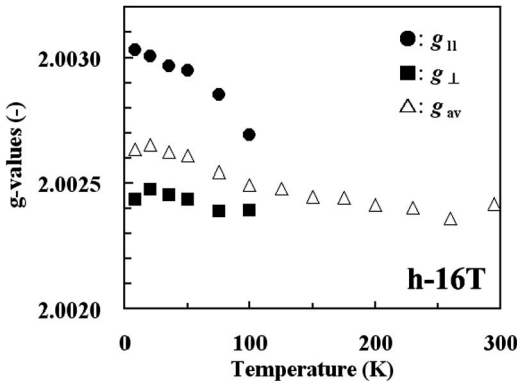

FIG. 4. Temperature dependences of $g_{\|}$, $g_{\perp}$, and g_{av} $[=1/3(g_{\|}+2\times g_{\perp})]$ for h-16T determined from spectral fits assuming an axially symmetric powder pattern below 100 K and an isotropic powder pattern above 100 K.

higher temperatures indicates that the electron spins transfer at the temperatures among several grains consisting of some chains. This is definite evidence that the electron spins, polarons, transfer between grains in the film. The result in the g anisotropy further suggests that such intergrain motions are activated by temperature. Conductivity of the doped conjugated polymers is known to increase with temperature and such feature is generally explained in terms of hopping processes with certain activation energy.[25] We emphasize that the intergrain motion of polarons activated by temperature should be one of decisive elements of the temperature dependence of conductivity.

The g factors of h-16T shown in Fig. 4 confirm that the spectra of h-16T are almost isotropic except at lower temperatures. Related to the interpretation about g anisotropy in o-20T, a feature of the quasi-isotropic g factor in h-16T probably stems from its amorphous morphology and this would be a common feature of amorphous conjugated polymer. In fact, observations of explicit g anisotropy have not been reported for amorphous type of heavily doped conjugated polymers, except for the case of the flat films of PATs that have some orientation.[24] Figure 4 also shows that the mean g values g_{av} in h-16T are almost temperature independent analogously to the result of o-20T. The g_{av} values of both oligomers, close to that of the free electron g_e (2.0023), indicate that their unpaired electrons originate from the π electrons. It is, however, noted that g_{av} of o-20T (2.0018–2.0020) is smaller than that of h-16T (2.0024–2.0026) and they are across g_e. A g value in the i direction can generally be calculated by the following equation:[26]

$$g_i = g_e - \sum_{n\neq 0} \frac{2\bar{\lambda}_n}{E_n - E_0}, \tag{1}$$

where E_0 is the energy of unpaired electrons before perturbation by the spin-orbit coupling (SOC), E_n is the energy of orbitals mixed through SOC, and $\bar{\lambda}_n$ is the SOC constant averaged over constituent atoms in the n orbital. This equation indicates that the relations $g<g_e$ and $g>g_e$ are obtained by the mixture of the unperturbed 0 orbital with its upper and lower levels, respectively. The result $g>g_e$ observed in

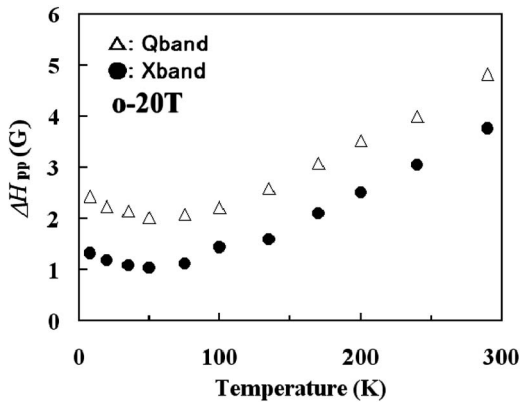

FIG. 5. Temperature dependences of the peak-to-peak Lorentzian linewidth $\Delta H_{p.p.}$ in *X*- and *Q*-band measurements for *o*-20T determined from spectral fits.

h-16T is thus characteristic of *p*-doped materials and has actually been reported on *p*-doped polypyrroles (PPy)[10,27] and PT derivatives.[28–32] Similarly, a *g* value smaller than g_e is typically observed in *n*-doped materials. Indeed, the electrochemically *n*-doped PT derivatives were reported to have *g* values smaller than g_e.[32] In this respect, the g_{av} values of *p*-doped *o*-20T, being smaller than g_e, are somewhat unexpected. Similar features in *g* values were also reported for some *p*-doped PATs with some crystalline morphology.[24] Therefore the features of g_{av} values smaller than g_e in *p*-doped conjugated polymers are presumably characteristic of a system with crystalline phases. The reason for it is not wholly understood at present, but we conjecture that delocalization is enhanced by the crystalline structure and it leads filled or vacant levels to being located just above unpaired polaron levels.

Figures 5 and 6 show temperature dependences of the *Q*- and *X*-band peak-to-peak Lorentzian linewidth $\Delta H_{p.p.}$ of *o*-20T and *h*-16T, respectively, derived from the spectral simulations. Both of the oligomers show a trend for $\Delta H_{p.p.}$ to increase with temperature. This feature, observed in most of heavily doped conjugated polymers,[10,33] has been explained to be caused by phonon scattering of spins (Elliott mechanism[34,35]) or by hopping of spins[36] via SOC. In these mechanisms (called "Elliott-like" mechanism, hereafter),

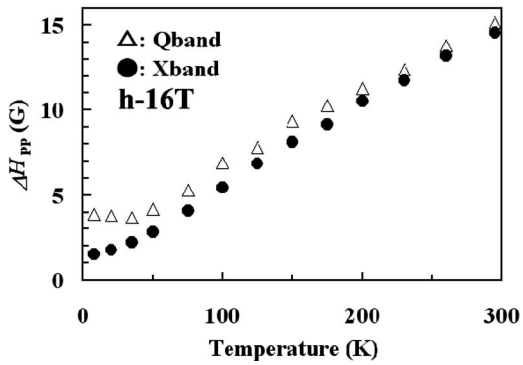

FIG. 6. Temperature dependences of the peak-to-peak Lorentzian linewidth $\Delta H_{p.p.}$ in *X*- and *Q*-band measurements for *h*-16T determined from spectral fits.

both forward and backward scatterings (hops) are known not to work effectively.[37–40] The inclusion of the Elliott-like behavior thus indicates that there exist effective scattering or hopping events perpendicular to a one-dimensional chain axis in both oligomers. The comparison between Figs. 5 and 6 suggests that $\Delta H_{p.p.}$ of *h*-16T is larger as a whole than that of *o*-20T. However, the magnitude of $\Delta H_{p.p.}$ at higher temperatures varied widely among different batches of samples in both oligomers and *h*-16T sometimes gave smaller $\Delta H_{p.p.}$ than *o*-20T. Such dispersion of $\Delta H_{p.p.}$ values stems from the Elliott-like term. We attribute the dispersion of the Elliott-like term to the morphological difference around polaron spins among different batches of samples.

IV. DISCUSSIONS

A. Origin of observed electron spin dynamics

In advance of discussions on the dynamics of the observed ESR signals, it should be clarified whether observed electron spins are dynamical or static. One of the most straightforward evidences that they are dynamical is the absence of electron spin echo (ESE) signals, because the ESE signals disappear when the resonance positions of individual spin components alter during either a dephasing or refocusing period due to their motion. The ESE signals are detected through a pulsed ESR measurement.[41] The absence of ESE signals was previously reported on PPy[42] and recently identified for *o*-20T as well.[18] This means that the ESR signals observed in *o*-20T are dynamical. Another evidence of being dynamical spins is Lorentzian line shape with no hyperfine splitting, because a rapid spin motion readily averages the hyperfine interaction. Such feature of line shape has been identified in the previous section by the spectral simulations for *h*-16T as well as *o*-20T. We therefore conclude that the observed ESR signals in the two oligomers originate from dynamical spins. Such dynamical properties of the spins allow the ESR spectrum to be motionally narrowed.

In *h*-16T with amorphous morphology, elements causing dynamical features of the spins are intra- and interchain motions. The contribution of these motions to ESR spectra can essentially be distinguished through the analyses of its ESR line shape.[4] However, the observed feature of Lorentzian line shape in 16T indicates that both intra- and interchain motions are so rapid as to cause motional narrowing and hence that their contributions are not distinguishable. The fact that the interchain spin motion in *h*-16T are rapid also appears in its *g* factor. In the previous section, *h*-16T was shown to have quasi-isotropic *g* factors. Previously, Krinichnyi and Roth showed using a *D*-band (140 GHz) ESR technique that nondoped and slightly doped PATs have appreciable *g* anisotropy.[43] This suggests that, if the spins in *h*-16T are not dynamical or move only along the chain axis, its *g* factors should exhibit anisotropy. The quasi-isotropic feature of *g* factors in *h*-16T is thus caused by such a rapid interchain motion as averages its inherent *g* anisotropy. This consequence should generally be true for amorphous type of doped conjugated polymers.

In contrast, *o*-20T gave anisotropic ESR spectra attributed to *g* anisotropy. This anisotropy does not stem from localized

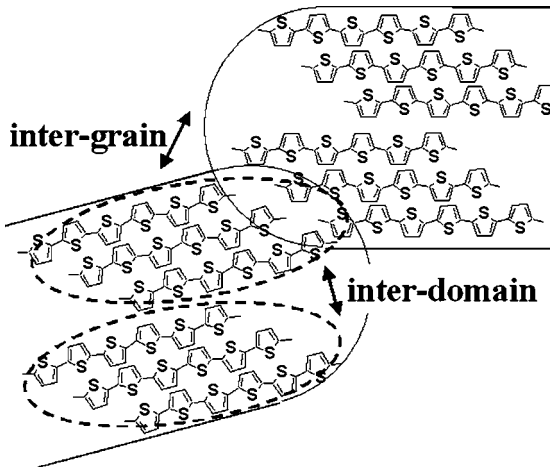

FIG. 7. Schematic representation of grain and domain structures expected in *o*-20T. The interfaces of the grain and the domain are represented by solid and broken curves, respectively. The intergrain and interdomain motions are represented by arrows. Dopant iodine anions are omitted for simplicity.

spins, because the observed ESR signals in *o*-20T are dynamical enough to give motional narrowing. In this case, a possible explanation is only that polaron spins spend most of the time at crystalline grains while moving within the grains. The spin is considered to originally delocalize at a confined domain in the grain. Then the interdomain motion in the grain would be the main element to give dynamical feature of signals, see Fig. 7. Most of the domains within the grain are expected to have the same g anisotropy, leading to the observation of powder-patterned ESR spectra with g anisotropy. Furthermore, the intergrain motion can also be present and is enhanced with increasing temperature, resulting in reduction of g anisotropy, as seen in Fig. 3. From these points, in crystalline *o*-20T, interdomain and intergrain motions determine its spin dynamics that is represented by behaviors of linewidth.

B. Polaron dynamics derived from the difference of ESR linewidth between *X*- and *Q*-band measurements

In the Results section, it was identified that the magnitude of Lorentzian linewidth $\Delta H_{p.p.}$ of both *h*-16T and *o*-20T is different between the *X*- and *Q*-band measurements (Figs. 5 and 6). In this section, the origin of the difference of $\Delta H_{p.p.}$ is discussed using a simplified model, and thereby we attempt to draw the information on the polaron dynamics in both oligomers.

As described in the previous section, we can regard observed ESR signals of both oligomers as originating from dynamical spins. This assures that the spectral line shape excluding the contribution of g anisotropy is homogeneous. In this case, the spin-spin relaxation time T_2^* determined from the inverse of $\Delta H_{p.p.}$ can be equal to the essential spin-spin relaxation time T_2.[42] The homogeneous linewidth $\Delta H_{p.p.}$ can then be assumed to compose of the term ΔH_e attributed to the Elliott-like behavior and the term ΔH_{mn} attributed to the motional narrowing effect (MNE) as follows:

$$\Delta H_{p.p.} = \Delta H_e + \Delta H_{\mathrm{mn}}. \tag{2}$$

The Elliott-like term does not depend on the magnitude of the Zeeman interaction. Hence its contribution is not expected to vary with the resonance frequency. This means that the difference of $\Delta H_{p.p.}$ between *X*- and *Q*-band measurements observed in *h*-16T and *o*-20T is not caused by the Elliott-like term. Therefore a change in the MNE term must be responsible for the $\Delta H_{p.p.}$ difference. ΔH_{mn} in Eq. (2), proportional to the spin-spin relaxation rate due to MNE $1/T_{2,\mathrm{mn}}$, is generally represented by the following formula:[44–46]

$$\Delta H_{\mathrm{mn}} \propto \frac{1}{T_{2,\mathrm{mn}}} = \gamma_e^2 h^2 [\phi(0) + \phi(\omega)]. \tag{3}$$

Here γ_e is the electron gyromagnetic ratio and h^2 is the mean square field that fluctuates with spin motions. This field is assumed to be isotropic since the observed ESR spectra can be represented by a powder pattern. Also $\phi(\omega)$ is the Fourier transform of the autocorrelation function $g(t)$. Physically, this formula means that the fluctuation of magnetic interaction is caused by spin motions expressed by $g(t)$. We here adopt an exponential type of autocorrelation function. This treatment is suitable for a nonanisotropic spin motion and its validity was actually confirmed for PPy[9] and *o*-20T.[18] Under this treatment, $\phi(\omega)$ is obtained as

$$\phi(\omega) = \frac{\tau_c}{1 + \omega^2 \tau_c^2}, \tag{4}$$

where τ_c is the correlation time and its inverse is a measure of hopping rate of electron spins. In this case, spin dynamics is simply represented by the single parameter τ_c that averages over different directions of motion, e.g., parallel and perpendicular directions along the chain axis.

We now consider the difference of linewidth between the *Q*- and *X*-band measurements. Among some possible magnetic interactions, only the Zeeman interaction can be the origin of the fluctuating field varying with the resonance frequency. Then, the linewidth difference for the variation of the resonance frequency ω is obtained from Eqs. (3) and (4) as follows:

$$\Delta(\Delta H_{p.p.})_{Q\text{-}X} \propto \Delta\left(\frac{1}{T_{2,\mathrm{mn}}}\right)_{Q\text{-}X} = \Delta\left[\gamma_e^2 h_g^2 \left(\tau_{c,g} + \frac{\tau_{c,g}}{1 + \omega^2 \tau_{c,g}^2}\right)\right]_{Q\text{-}X}, \tag{5}$$

where the expression $\Delta(a)_{Q\text{-}X}$ represents the difference of quantity a between the *Q*- and *X*-band measurements. The correlation time $\tau_{c,g}$ is defined for the fluctuation of the isotropic squared Zeeman filed h_g^2 that is proportional to the squared g anisotropy $(g_\parallel - g_\perp)^2$. In the case of slow spin motions $(1 < \omega^2 \tau_{c,g}^2)$, the first term in the right hand side of Eq. (5) is larger than the second one. Further, the second term is approximated as $\gamma_e^2 h_g^2 / \omega^2 \tau_{c,g}$ and it is independent of ω because h_g^2, proportional to the squared g-anisotropy $(g_\parallel - g_\perp)^2$, and ω^2 have the same frequency dependence. In the case of fast spin motions $(1 > \omega^2 \tau_{c,g}^2)$, the second term gets close to

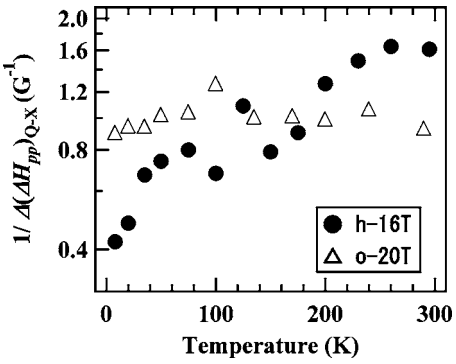

FIG. 8. Plots of the inverse of the $\Delta H_{p.p.}$ difference between X- and Q-band measurements $[\Delta(\Delta H_{p.p.})_{Q\text{-}X}]$ for h-16T and o-20T versus temperature.

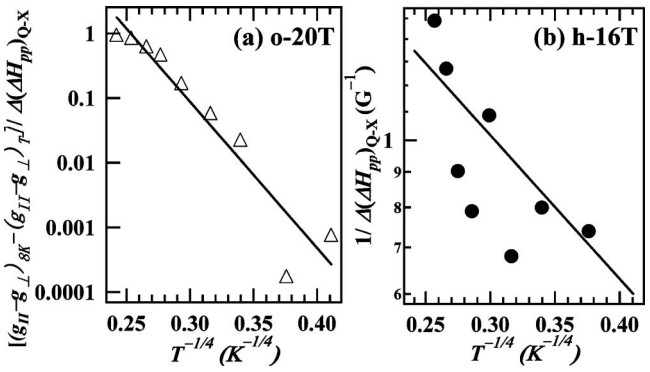

FIG. 9. Plots of (a) $[(g_{\parallel}-g_{\perp})_{8\ \mathrm{K}}-(g_{\parallel}-g_{\perp})_{T}]^2/\Delta(\Delta H_{p.p.})_{Q\text{-}X}$ (arbitrary units) in o-20T and (b) $1/\Delta(\Delta H_{p.p.})_{Q\text{-}X}$ in h-16T versus $T^{-1/4}$ (T: temperature). The solid lines in the figures are results of linear fits.

the first one and the sum of them is $2\gamma_e^2 h_g^2 \tau_{c,g}$ at most. Therefore, eventually, $\Delta(\Delta H_{p.p.})_{Q\text{-}X}$ in Eq. (5) is determined by the term $\gamma_e^2 \tau_{c,g} \Delta(h_g^2)_{Q\text{-}X}$. This indicates that the information on the spin dynamics, $1/\tau_{c,g}$, can be obtained by the inverse of $\Delta(\Delta H_{p.p.})_{Q\text{-}X}$.

Temperature dependences of the inverse of $\Delta(\Delta H_{p.p.})_{Q\text{-}X}$ in h-16T and o-20T are shown in Fig. 8. In h-16T, both interchain and intrachain motions are possible elements of MNE. However, the term $\Delta(h_g^2)_{Q\text{-}X}$ must be determined by the interchain motion. This is because the intrachain motion, probably dominated by transfers between segments parallel to each other, is expected to cause much less fluctuation of the Zeeman field than the interchain motion. In addition, the g factors of h-16T shown in Fig. 4 suggest that the temperature variation of $\Delta(h_g^2)_{Q\text{-}X}$ is small. Therefore the temperature dependence of $1/\Delta(\Delta H_{p.p.})_{Q\text{-}X}$ in h-16T is determined by that of the interchain correlation rate $1/\tau_{c,g}$. From a similar argument, with respect to o-20T, the Zeeman fluctuating field in the intergrain motion should be much larger than the case in the intragrain motion as well as the interchain one. Then the temperature dependence of the squared Zeeman field h_g^2 that fluctuates with the intergrain motion can be estimated as follows, based on the result of g anisotropy obtained in Fig. 3:

$$h_g^2 \propto [(g_{\parallel}-g_{\perp})_{8\ \mathrm{K}}-(g_{\parallel}-g_{\perp})_{T}]^2. \tag{6}$$

Here, the Zeeman fluctuating field is assumed to be the minimum at 8 K (the lowest measurement temperature). Therefore, finally, the temperature dependence of the correlation rate $(1/\tau_{c,g})$ for the intergrain motion in o-20T is obtained by the calculation $[(g_{\parallel}-g_{\perp})_{8\ \mathrm{K}}-(g_{\parallel}-g_{\perp})_{T}]^2/\Delta(\Delta H_{p.p.})_{Q\text{-}X}$.

From these arguments, the temperature dependences of interchain and intergrain hopping rates $(1/\tau_{c,g})$ can be investigated by the terms $1/\Delta(\Delta H_{p.p.})_{Q\text{-}X}$ in h-16T and $[(g_{\parallel}-g_{\perp})_{8\ \mathrm{K}}-(g_{\parallel}-g_{\perp})_{T}]^2/\Delta(\Delta H_{p.p.})_{Q\text{-}X}$ in o-20T, respectively. We here analyze these hopping behaviors with the variable range hopping (VRH) model,[47] typically used for explaining hopping transport in amorphous semiconductors including conjugated polymers.[25,48,49] Hopping transport following the VRH model is usually confirmed by the temperature dependence of $\exp[-(T_0/T)^{1/4}]$ type for a three-dimensional transport. Such temperature dependences were indeed reported on the conductivity of heavily doped PAT.[49–51] Plots of $1/\Delta(\Delta H_{p.p.})_{Q\text{-}X}$ for h-16T and $[(g_{\parallel}-g_{\perp})_{8\ \mathrm{K}}-(g_{\parallel}-g_{\perp})_{T}]^2/\Delta(\Delta H_{p.p.})_{Q\text{-}X}$ for o-20T versus $T^{-1/4}$ are shown in Fig. 9. First, the result in o-20T demonstrates that its intergrain hopping process almost follows the VRH model. This result is interesting because a hopping process following the VRH model has been identified from a microscopic view using an ESR technique. T_0 obtained from the best fit is 7.4×10^6 K. This value is not far from the previously reported T_0 values $[(1.4-2.8)\times10^7\ \mathrm{K}]$ obtained from conductivity measurements for head-to-tail coupled PATs that have crystalline morphology.[49] This suggests that the temperature dependence of conductivity in the conjugated polymers with a crystalline morphology should be dominated by this type of intergrain hopping process of polarons.

In contrast, plots for h-16T in Fig. 9 suggest that the temperature dependence of $1/\tau_{c,g}$ (interchain hopping rates) does not follow well the VRH model. In fact, T_0 estimated roughly from the plots is 5.2×10^2 K and much smaller than T_0 of o-20T. This is somewhat unexpected because temperature dependences of conductivity are expected to be similar between h-16T and o-20T since their conductivities at room temperature were in the same orders of magnitude. This T_0 difference between h-16T and o-20T could merely be due to a difference in the hopping process between the interchain and intergrain ones. As another possible explanation, events such as phonon scattering of the spins causing the Elliott mechanism could be somewhat involved in the temperature dependence of $1/\tau_{c,g}$ for h-16T, because spin motions via this event can also give rise to MNE, and because this event is expected to have much weaker temperature dependence than a hopping process. It could be difficult to reach a conclusion at this stage about the origin of observed spin dynamics in 16T but we shall finally emphasize that this result in h-16T could reflect an intrinsic interchain polaron dynamics. This is because conductivity can be determined by less efficient hops at minor sites, while the ESR information is a result averaged over several sites that could have different spin dynamics.

V. CONCLUSIONS

The polaron dynamics was investigated for the two types of long oligothiophenes, *o*-20T and *h*-16T, through the *X*- and *Q*-band ESR measurements. *o*-20T, used as a model of conjugated polymers with crystalline grains, gave anisotropic ESR spectra originating from *g* anisotropy at low temperatures. The anisotropy is concluded to be caused by polarons that move within grains consisting of parallel chains. Also the anisotropy was shown to decrease with increasing temperature. The decrease of *g* anisotropy is concluded to stem from the transfer of polarons among several grains. This is definite experimental evidence that polarons in doped conjugated polymers transfer between grains in the film. In contrast, *h*-16T, used as a model of the polymers with amorphous morphology, gave almost isotropic ESR spectra. The anisotropic and isotropic features in ESR line shape are concluded to be characteristic of polymer samples with crystalline and amorphous morphologies, respectively. The ESR spectra of two oligomers were fitted well using axially symmetric *g* factors and a Lorentzian linewidth. The fitting results showed that the mean *g* values of *o*-20T are smaller than that of *h*-16T. We concluded that smaller g_{av} values than g_e identified in *o*-20T should be characteristic of a system with crystalline phases.

Both of the oligomers showed a trend for the linewidth to increase with temperature, called the Elliott-like behavior. In addition, the linewidth was shown to be larger in the *Q*-band measurement in both oligomers. The difference of the linewidth was analyzed by the motional narrowing model and concluded to be caused primarily by the intergrain motion in *o*-20T and by the interchain motion in *h*-16T. The analysis for *o*-20T eliminating the contribution of the *g* anisotropy showed that the intergrain motion almost follows the VRH model. The interchain motion in *h*-16T, in contrast, was shown to have a much weaker temperature dependence than the intergrain motion in *o*-20 T. This difference was concluded to be due to the presence of several processes in the interchain motion that can contribute to the motional narrowing effect. We emphasize that the analyses performed on the basis of the linewidth difference between different frequency measurements are effective ways to investigate the polaron dynamics associated with conductivity.

ACKNOWLEDGMENTS

We thank M. Maruyama and H. Hashimoto at Osaka City University for assisting in XRD measurements.

*Author to whom correspondence should be addressed. FAX: +81-6-6605-2522; kkane@sci.osaka-cu.ac.jp

[1] H. Sirringhaus, P. J. Brown, R. H. Friend, M. M. Nielsen, K. Bechgaard, B. M. W. Langeveld-Voss, A. J. H. Spiering, R. A. J. Janssen, E. W. Meijer, P. Herwig, and D. M. de Leeuw, Nature (London) **401**, 685 (1999).

[2] R. Menon, in *Handbook of Organic Conductive Molecules and Polymers*, edited by H. S. Nalwa (Wiley, Sussex, 1997), p. 47.

[3] K. Mizoguchi and S. Kuroda, in *Handbook of Organic Conductive Molecules and Polymers*, edited by H. S. Nalwa (Wiley, Sussex, 1997), p. 251.

[4] M. Nechtschein, in *Handbook of Conducting Polymers II*, edited by T. A. Skotheim, R. L. Elsenbaumer, and J. R. Reynolds (Dekker, New York, 1997), p. 141.

[5] X. Wei, B. C. Hess, and Z. V. Vardeny, Phys. Rev. Lett. **68**, 666 (1992).

[6] L. S. Swanson, J. Shinar, A. R. Brown, D. D. C. Bradley, R. H. Friend, P. L. Burn, A. Kraft, and A. B. Holmes, Phys. Rev. B **46**, 15072 (1992).

[7] V. Dykanov, N. Gauss, G. Rosler, S. Karg, and W. Riess, Chem. Phys. **189**, 687 (1994).

[8] K. Holczer, J. P. Boucher, F. Devreux, and M. Nechtschein, Phys. Rev. B **23**, 1051 (1981).

[9] K. Kanemoto and J. Yamauchi, Phys. Rev. B **61**, 1075 (2000).

[10] K. Kanemoto and J. Yamauchi, Synth. Met. **114**, 79 (2000).

[11] G. Schopf and G. Kossmehl, *Polythiophenes-Electrically Conductive Polymers* (Springer, Berlin, 1997).

[12] *Handbook of Oligo- and Polythiophenes*, edited by D. Fichou (Wiley-VCH, Weinheim, 1999).

[13] T. Otsubo, Y. Aso, and K. Takimiya, Bull. Chem. Soc. Jpn. **74**, 1789 (2001).

[14] H. Nakanishi, N. Sumi, Y. Aso, and T. Otsubo, J. Org. Chem. **63**, 8632 (1998).

[15] N. Sumi, H. Nakanishi, S. Ueno, K. Takimiya, Y. Aso, and T. Otsubo, Bull. Chem. Soc. Jpn. **74**, 979 (2001).

[16] H. Nakanishi, N. Sumi, S. Ueno, K. Takimiya, Y. Aso, T. Otsubo, K. Komaguchi, M. Shiotani, and N. Ohta, Synth. Met. **119**, 413 (2001).

[17] K. Kanemoto, T. Sudo, I. Akai, H. Hashimoto, T. Karasawa, Y. Aso, and T. Otsubo, Phys. Rev. B **73**, 235203 (2006).

[18] K. Kanemoto, T. Kato, Y. Aso, and T. Otsubo, Phys. Rev. B **68**, 092302 (2003).

[19] K. Takimiya, K. Sakamoto, T. Otsubo, and Y. Kunugi, Chem. Lett. **35**, 942 (2006).

[20] T. J. Prosa, M. J. Winokur, J. Moulton, P. Smith, and A. J. Heeger, Synth. Met. **55-57**, 370 (1993).

[21] T. A. Chen, X. M. Wu, and R. D. Rieke, J. Am. Chem. Soc. **117**, 233 (1995).

[22] E. Houze and M. Nechtschein, Phys. Rev. B **53**, 14309 (1996).

[23] K. Kanemoto and J. Yamauchi, J. Phys. Chem. B **105**, 2117 (2001).

[24] D. W. Breiby, S. Sato, E. J. Samuelsen, and K. Mizoguchi, J. Polym. Sci., Part B: Polym. Phys. **41**, 3011 (2003).

[25] E. M. Conwell, in *Handbook of Organic Conductive Molecules and Polymers*, edited by H. S. Nalwa (Wiley, Sussex, 1997), p. 1.

[26] J. A. Weil, J. R. Bolton, and J. E. Wertz, *Electron Paramagnetic Resonance: Elementary Theory and Practical Applications* (Wiley, New York, 1994).

[27] J. C. Scott, P. Pfluger, M. T. Krounbi, and G. B. Street, Phys. Rev. B **28**, 2140 (1983).

[28] G. Tourillon, D. Gourier, P. Garnier, and D. Vivien, J. Phys.

Chem. **88**, 1049 (1984).
[29] H. L. Bandey, P. Cremins, S. E. Garner, A. R. Hillman, J. B. Raynor, and A. D. Workman, J. Electrochem. Soc. **142**, 2111 (1995).
[30] Y. Harima, T. Eguchi, K. Yamashita, K. Kojima, and M. Shiotani, Synth. Met. **105**, 121 (1999).
[31] X. Jiang, R. Patil, Y. Harima, J. Ohshita, and A. Kunai, J. Phys. Chem. B **109**, 221 (2005).
[32] F. Lafolet, F. Genoud, B. Divisia-Blohorn, C. Aronica, and S. Guillerez, J. Phys. Chem. B **109**, 12755 (2005).
[33] K. Mizoguchi, M. Honda, N. Kachi, F. Shimizu, H. Sakamoto, K. Kume, S. Masubuchi, and S. Kazama, Solid State Commun. **96**, 333 (1995).
[34] R. J. Elliott, Phys. Rev. **96**, 266 (1954).
[35] Y. Yaffet, in *Solid State Physics*, edited by H. Ehrenreich, F. Seitz, and D. Turnbull (Academic, New York, 1963), Vol. 14, p. 1.
[36] O. Chauvet, S. Paschen, M. N. Bussac, and L. Zuppiroli, Europhys. Lett. **26**, 619 (1994).
[37] D. Jerome and H. Schultz, Adv. Phys. **31**, 299 (1982).
[38] C. Coulon and R. Clérac, Chem. Rev. (Washington, D.C.) **104**, 5655 (2004).
[39] H. J. Pedersen, J. C. Scott, and K. Bechgaard, Phys. Rev. B **24**, 5014 (1981).
[40] M. Krebs, W. Bietsch, J. U. von Schütz, and H. C. Wolf, Synth. Met. **64**, 187 (1994).
[41] A. Schweiger, Angew. Chem., Int. Ed. Engl. **30**, 265 (1991).
[42] K. Kanemoto and J. Yamauchi, Appl. Magn. Reson. **18**, 227 (2000).
[43] V. I. Krinichnyi and H. K. Roth, Appl. Magn. Reson. **26**, 395 (2004).
[44] A. Abragam, *Principles of Nuclear Magnetism* (Clarendon, Oxford, 1961).
[45] A. Carrington and A. D. McLachlan, *Introduction to Magnetic Resonance* (Harper and Row, New York, 1967).
[46] C. P. Slichter, *Principles of Magnetic Resonance* (Springer-Verlag, Berlin, 1990).
[47] N. F. Mott and E. A. Davis, *Electronic Processes in Noncrystalline Materials* (Oxford University Press, London, 1979).
[48] A. K. Meikap, A. Das, S. Chatterjee, M. Digar, and S. N. Bhattacharyya, Phys. Rev. B **47**, 1340 (1993).
[49] C. O. Yoon, M. Reghu, D. Moses, A. J. Heeger, Y. Cao, T.-A. Chen, X. Wu, and R. D. Rieke, Synth. Met. **75**, 229 (1995).
[50] T. Yamamoto, M. Abla, T. Shimizu, D. Komarudin, B.-L. Lee, and E. Kurokawa, Polym. Bull. (Berlin) **42**, 321 (1999).
[51] S. Ukai, H. Ito, K. Marumoto, and S. Kuroda, J. Phys. Soc. Jpn. **74**, 3314 (2005).